ELSEVIER

Journal of Photochemistry and Photobiology
A: Chemistry 88 (1995) 117–123

Journal of PHOTOCHEMISTRY AND PHOTOBIOLOGY A:CHEMISTRY

Properties of singlet excited *N*-(pyrimidin-2-one-4-yl)pyridinium chloride and structurally related organic cations

G. Wenska, B. Skalski, J. Koput, S. Paszyc

Faculty of Chemistry, A. Mickiewicz University, Poznan, Poland

Received 17 November 1994; accepted 26 January 1995

Abstract

The UV absorption and fluorescence spectra, fluorescence quantum yields and lifetimes of four new fluorescent *N*-(pyrimidin-2-one-4-yl)pyridinium and *N*-(pyrimidin-2-one-4-yl)methylimidazolium cations were measured in several solvents at room temperature and in ethanol glasses at 77 K. The spectroscopic studies were supplemented by theoretical calculations of the electronic transition energies, oscillator strengths and dipole moment changes by the INDO/S CI method. It is concluded that the lowest excited singlet state of the compounds studied has charge transfer character. The significantly different charge distribution in the S_1 state and the rotational relaxation of the excited molecules are responsible for the large Stokes shift observed in the spectra of pyridinium cations. *N*-(Pyrimidin-2-one-4-yl)methylimidazolium cations are more efficient fluorophores than pyridinium cations and this is due to the increased rate of non-radiative decay in the latter compounds.

Keywords: Singlet excited state; Organic cations; UV absorption; Fluorescence spectra; Fluorescence quantum yields; Lifetimes

1. Introduction

The photophysical processes in singlet excited *N*-heteroaromatic cations have been the subject of numerous reports [1–8] over the last two decades. In particular the fluorescence properties of *N*-aryl-substituted pyridinium species have been studied in detail [3,5]. We have recently described the photophysical properties of several *N*-(purin-9-yl)pyridinium chlorides [9,10]. Our interest in these compounds stems from the fact that they are fluorescent derivatives of nucleic acid bases. As we have already shown, the chemical transformations of common purine and pyrimidine bases into fluorescent pyridinium derivatives occur under mild reaction conditions [11,12] and can be performed on oligonucleotides resulting in the formation of intrinsic fluorophores [13]. In order to estimate the potential use of these new fluorescent derivatives as probes in nucleic acids, we have undertaken a systematic study of their photophysical properties.

In this paper, we report the results of the UV absorption and emission spectroscopy and theoretical studies of pyridinium compounds **1** and **2** (Scheme 1) derived from pyrimidine bases. The results concerning structurally related *N*-(pyrimidin-2-one-4-yl)methylimidazolium chlorides **3** and **4** (Scheme 1) are also presented.

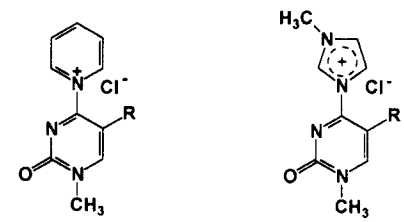

1 R = H
2 R = CH_3

3 R = H
4 R = CH_3

Scheme 1.

2. Experimental details

2.1. Materials

All the organic solvents were of spectroscopic, fluorescence (Merck) or high performance liquid chromatography (HPLC) (Aldrich) grades and were used as received. Water was purified using a Millipore Super-Q system. Fluorescence emission from the solvents was found to be insignificant. Compounds **1–4** were synthesized as described previously [12]. When necessary,

1010-6030/95/$09.50
SDI 1010-6030(95)04051-X

particularly after prolonged storage, they were purified by chromatography on a silica gel column. Acetonitrile followed by a mixture of CH_3CN and 0.1 N aqueous HCl (5:1) were used as eluents in the case of compounds **1** and **2** and a mixture of CH_3CN and 30% aqueous acetic acid was used as the eluent in the case of compounds **3** and **4**. The eluates were concentrated under vacuum (temperature, less than 35 °C), neutralized with ion exchange resin (HCO_3^- form), passed through ion exchange resin (Cl^- form) and freeze dried to give the solid samples of **1–4**. Prior to use, the purity of all the compounds was checked by HPLC analysis (Waters-Millipore) employing photodiode array absorption and fluorescence detectors. The analyses were performed on a reversed phase Delta Pak C-4 column eluted with a gradient of CH_3CN in 0.1 M aqueous ammonium acetate.

2.2. Methods

Absorption spectra were recorded with a Perkin–Elmer Lambda 17 UV–visible spectrophotometer and fluorescence spectra were recorded using Perkin–Elmer MPF-66 and LS-50 B spectrofluorometers. Fluorescence quantum yields were determined using quinine sulphate in 0.1 M H_2SO_4 as a standard ($\phi_f = 0.51$) [14]. Fluorescence lifetimes were measured using the time-correlated single-photon-counting technique [15] with a model 5000 fluorescence lifetime spectrophotometer (IBH Consultants) [16]. Reconvolution of fluorescence decay curves was performed using the IBH Consultants version 4 software. Low temperature (77 K) emission and excitation spectra were measured in ethanol glasses in a quartz tube of 5 mm path length using a quartz Dewar cold finger assembly.

3. Results and discussion

3.1. Absorption and fluorescence in aqueous solution

The UV absorption spectra of compounds **1** and **3** in water are presented in Figs. 1 and 2 respectively. In the case of **1**, two absorption bands appear in the spectrum at about 260 and 330 nm, whereas in the case of **3** only one absorption band appears in the near-UV region at 313 nm. Compounds **1–4** can be regarded as intramolecular electron donor–acceptor systems, pyridinium and methylimidazolium residues being the acceptor and the pyrimidin-2-one-4-yl residue the donor. Therefore the lowest energy bands in the absorption spectra of **1–4** are due to the intramolecular charge transfer (CT) interaction in these compounds. As expected for CT absorption, the position of the band maximum depends on the ionization energy of the electron donor and the electron affinity of the

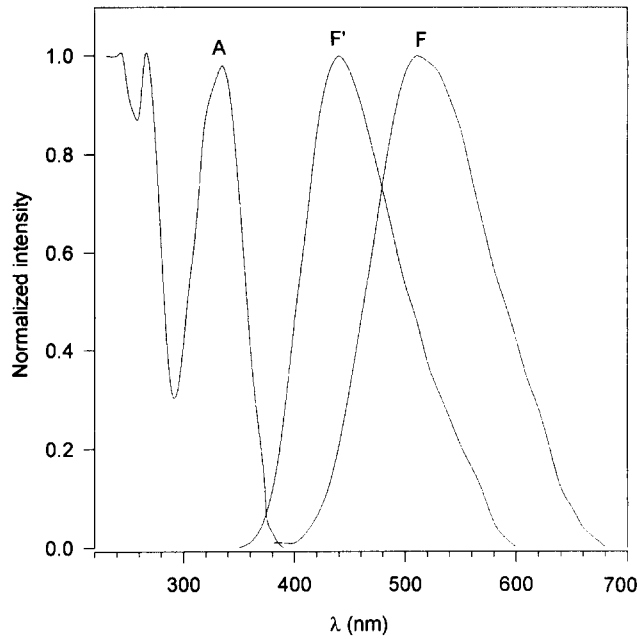

Fig. 1. Normalized room temperature absorption (A) and fluorescence emission (F) spectra of compound **1** in aqueous solution and low temperature (77 K) fluorescence (F') spectrum in ethanol glass.

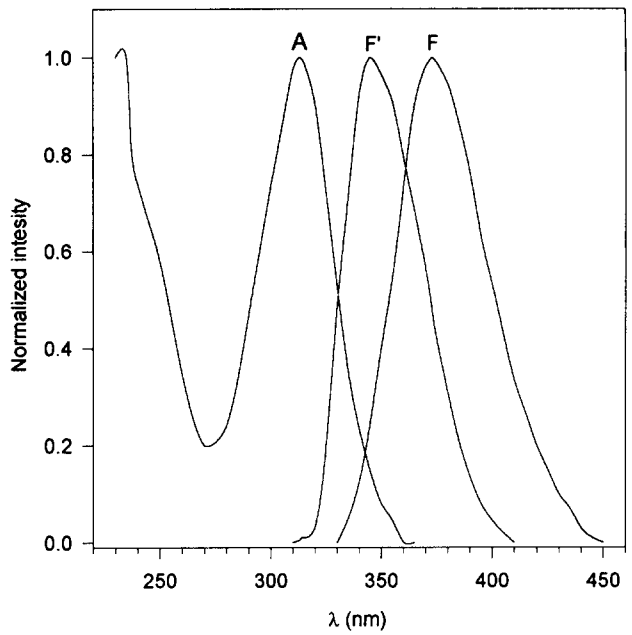

Fig. 2. Normalized room temperature absorption (A) and fluorescence emission (F) spectra of compound **3** in aqueous solution and low temperature (77 K) fluorescence (F') spectrum in ethanol glass.

electron acceptor. Thus replacing the pyridinium residue in compound **1** with methylimidazolium (in compound **3**) shifts the 329 nm band to 313.5 nm. On the other hand, a red shift of the long-wavelength absorption band is observed in the UV spectrum on introduction of a methyl substituent into the pyrimidinone ring. As indicated by the data in Table 1, this effect is more pronounced in methylimidazolium derivatives than in compounds containing pyridinium residues

Table 1
Absorption and fluorescence data for compounds 1–4 in aqueous solution

	1	2	3	4
UV absorption				
$\lambda_{a,max}$ (nm)	329	333	313.5	324
ϵ (M^{-1} cm^{-1})	6500	5000	4800	4700
$\Delta\nu_{a,1/2}$ (cm^{-1})	4350	4200	3850	3850
Fluorescence				
$\lambda_{f,max}$ (nm)	510	546	373	389
$\Delta\nu_{f,1/2}$ (cm^{-1})	4800	4900	3800	3900
ϕ	0.021	0.002	0.140	0.104
τ (ns)	0.8	0.1	3.7	3.5
k_f (10^7 s^{-1})	2.6	2.0	3.7	3.0
Σk_{nr} (10^8 s^{-1})	12.2	99.8	2.3	2.6
$\|M\|$ (D)	2.1	2.0	1.6	1.6
$\nu_{a,max} - \nu_{f,max}$ (cm^{-1})	10800	11700	5100	5200

($\nu_{a,max}(3) - \nu_{a,max}(4) = 1500$ cm^{-1}, $\nu_{a,max}(1) - \nu_{a,max}(2) = 800$ cm^{-1}).

Compounds **1–4** emit fluorescence at room temperature. The emission maxima, band halfwidths ($\Delta\nu_{f,1/2}$), quantum yields (ϕ) and lifetimes (τ) are presented in Table 1. Figs. 1 and 2 show the fluorescence spectra of compounds **1** and **3**. The fluorescence excitation spectra match the respective absorption spectra. The room temperature emission of all the compounds studied is characterized by a single, rather broad, structureless band. However, the location of the band strongly depends on the structure of the compound. The Stokes shift $\nu_{a,max} - \nu_{f,max}$ calculated for compounds **3** and **4** (Table 1) is nearly doubled for pyridinium cations **1** and **2**. *N*-(pyrimidin-2-one-4-yl)methylimidazolium derivatives (**3** and **4**) are much more efficient fluorophores than their pyridinium counterparts (**1** and **2**). The fluorescence quantum yields of the former are an order of magnitude higher than those of the latter. The fluorescence of compounds **1–4** shows monoexponential decay in the nanosecond region. The values of the rate constants for radiative (k_f) and non-radiative (Σk_{nr}) decay of the S_1 state, calculated from $k_f = \phi/\tau$ and $\Sigma k_{nr} = (1 - \phi/\tau)$ respectively, are included in Table 1. They show that the reduced yield of pyridinium derivatives is mainly due to the enhanced rate of non-radiative decay. The values of the transition dipole moment $|M|$ of the emitting state, calculated from the relation $k_f = 64\pi^4 n^3 \nu_f^3 |M|^2/3h$ [17], are comparable for all the compounds (Table 1) and indicate that the transitions have similarly allowed character.

It should be noted that the absorption and fluorescence characteristics of compounds **1–4** are insensitive to pH in aqueous solutions up to pH 1 and are also independent of concentration in the range 2×10^{-4} to 10^{-5} M. The fluorescence lifetimes τ are independent of the excitation and emission wavelength in aqueous solutions and the other solvents studied (see below).

3.2. Effect of the solvent

The dependence of the absorption and fluorescence spectra of compounds **1–4** on the solvent is summarized in Tables 2 and 3. The choice of solvent used for spectroscopic studies was limited by the insolubility of the highly polar, ionic compounds in organic solvents of moderate polarity.

The position of the 260 nm band in the UV spectrum of pyridinium cations in aqueous solution (Fig. 1) does not change with the solvent. On the other hand, the longest wavelength absorption band in the UV spectra of **1** and **2** as well as **3** and **4** shifts to the red on going from water to less polar organic solvents. Negative solvatochromism was previously observed in the UV spectra of *N*-(purinyl)pyridinium and other related ionic compounds and was interpreted in terms of the decreased polarity of the singlet excited state of these compounds [9,10,18]. The maximum of the fluorescence band changes to a lesser degree with the solvent, compared with the absorption maximum, but the same trend is observed. In all the solvents, the halfwidth of the fluorescence band remains approximately constant. The polarity is not the sole parameter which influences the spectral characteristics of these compounds. The correlation of the absorption and fluorescence maxima with the solvent parameters $f(D, n)$ defined by Lippert [19] and Bilot and Kawski [20] shows a non-linear behaviour. This indicates specific solute–solvent interactions, in particular hydrogen bonding. Hydrogen bond donor solvents (most probably to the O atom of the carbonyl group [21]) increase the ionization energy of the donor (pyrimidinone) moiety of the molecules. A hypsochromic shift of the absorption band is observed as a consequence. In order to determine the respective contributions of the polarity of the solvent and its hydrogen bonding ability in the observed spectral changes, we have applied the simplified Kamlet equation [22]

$$\nu = \nu_0 + s\pi^* + a\alpha$$

where ν is the wavenumber of the absorption (or emission) maximum, π^* is the solvent polarity parameter taken from Ref. [22] and α is the parameter describing the ability of the solvent to donate a proton in a solvent-to-solute H bond.

This approach was found to be suitable for the interpretation of solvent effects on the electronic transition energies in various organic compounds [8,23,24]. The results obtained from multiple linear regression analysis are presented in Table 4 and include the coefficients s and a, intercept (ν_0), standard deviation and multiple correlation coefficient (R). The results of

Table 2
UV absorption characteristics of compounds 1–4 in various solvents

Solvent	1	2	3	4
	$\lambda_{a,max}$ (nm) (ϵ)	$\lambda_{a,max}$ (nm) (ϵ)	$\lambda_{a,max}$ (nm) (ϵ)	$\lambda_{a,max}$ (nm) (ϵ)
Ethylene glycol	337 (5000)	338 (4600)	317 (4500)	329 (4600)
Methanol	336 (4900)	339 (4200)	318 (4300)	330 (4500)
Ethanol	337 (4800)	340 (4000)	319 (4400)	331 (4700)
2-Propanol	342 (4800)	342 (4000)	320 (4200)	332 (4300)
n-Butanol	342 (4600)	343 (4400)	321 (4100)	333 (4100)
Acetonitrile	341 (4800)	344 (4200)	323.5 (4600)	335.5 (4500)
Butyronitrile	345 (5200)	348 (4500)	325 (4600)	336 (4400)

Table 3
Fluorescence maxima ($\lambda_{f,max}$), quantum yields (ϕ) and lifetimes (τ) for compounds 1–4 in various solvents

Solvent	Compound	$\lambda_{f,max}$ (nm)	ϕ	τ (ns)
Ethylene glycol	1	514	0.011	0.9
	2	541	0.002	–[a]
	3	376	0.110	3.9
	4	392	0.088	3.6
Methanol	1	520	0.009	0.8
	2	548	0.002	–
	3	380	0.130	4.2
	4	397	0.109	4.2
Ethanol	1	524	0.010	–
	2	549	0.002	–
	3	381	0.076	2.4
	4	397	0.065	2.8
2-Propanol	1	523	0.008	–
	2	546	0.001	–
	3	383	0.076	2.8
	4	399	0.065	2.4
n-Butanol	1	522	0.006	–
	2	545	0.001	–
	3	384	0.084	2.9
	4	400	0.075	2.7
Acetonitrile	1	515	0.025	1.2
	2	542	0.002	0.1
	3	379	0.084	2.7
	4	396	0.077	2.8
Butyronitrile	1	520	0.019	1.0
	2	547	0.001	–
	3	381	0.078	2.7
	4	398	0.073	2.8

[a] Not determined. Fluorescence lifetimes τ of compounds 1 and 2 are shorter than 0.8 ns and 0.3 ns respectively.

the calculations are consistent with the qualitative observations presented above. Both the absorption and fluorescence energies of compounds **1** and **3** are influenced by specific solute–solvent interactions. However, the contribution of hydrogen bonding to the overall electronic energy changes, as measured by the ratio of the coefficients *a*/*s*, is much higher in the ground state than in the relaxed excited state for both compounds **1** and **3**. Breaking of the H bonds in the excited state is expected, since pyrimidinone will be electron deficient upon excitation. The increase in energy of the Franck–Condon ground state is probably the cause of the negative sign of the regression coefficient *a* in the correlation of the fluorescence maxima ν_f of compound **1** [23].

The fluorescence parameters (ϕ, τ) measured in selected solvents are included in Table 3. The fluorescence lifetimes of the methylimidazolium cations **3** and **4** are significantly longer than those for the pyridinium cations **1** and **2**. The values of k_f and Σk_{nr} for all the compounds in acetonitrile, which can be calculated from the experimental data presented in Table 3, are consistent with those found in aqueous solution and support the existence of an efficient channel of non-radiative decay in pyridinium cations, particularly in compound **2**.

3.3. Effect of temperature

The fluorescence spectra of **1** and **3** measured in ethanolic glasses at 77 K are presented in Figs. 1 and 2 respectively. A blue shift of 3600 cm^{-1} for **1** and 2700 cm^{-1} for **3** on going from fluid ethanol to rigid glass is observed. It is interesting to note that the large Stokes shift (6000 cm^{-1}) is retained in the spectrum of the *N*-(pyrimidin-2-one-4-yl)pyridinium cation **1** even under the conditions in which solvent reorientation and large amplitude molecular motions are inhibited [25]. No phosphorescence could be detected for pyridinium cation **1** in contrast with methylimidazolium cation **3** which emits phosphorescence with a maximum at 455 nm.

3.4. Fluorescence quenching

We examined the quenching of the fluorescence of compounds **1** and **3** by halide (Cl^-, Br^-, I^-) counterions

Table 4
The results of the multiple regression analysis of the Kamlet correlation of solvent spectral shifts

Compound	s (cm^{-1})	a (cm^{-1})	Intercept (cm^{-1})	R	Standard deviation
Absorption					
1	850(±210)	950(±220)	28350(±160)	0.95	±160
3	380(±40)	800(±100)	30490(±80)	0.99	±30
Fluorescence					
1	870(±40)	−110(±60)	18780(±20)	0.98	±40
3	1070(±60)	160(±30)	25450(±110)	0.98	±50

in aqueous solution at constant ionic strength ($NaClO_4$). The Stern–Volmer plots for the quenching of the fluorescence of compounds **1** and **3** by Br^-, constructed from steady state and lifetime measurements, are presented in Fig. 3. The plots $\phi^0/\phi - 1$ vs. [Q] show upward curvature at high concentrations of halide ions, the behaviour noted previously for *N*-(purinyl)pyridinium species [9,10]. The values of the quenching constants k_q ($\times 10^{10}$ M^{-1} s^{-1}), calculated from the linear plots of $\tau^0/\tau - 1$ vs. [Q], are equal to 1.1 (I^-), 0.9 (Br^-) and 0.2 (Cl^-) for **1** and 0.8 (I^-), 0.6 (Br^-) and 0.1 (Cl^-) for **3**. Although chloride ions were found to be fluorescence quenchers, no counterion effect [26] was observed in the solvent used. Both the absorption and fluorescence parameters for **1** and **3** in water and 2-propanol were identical within experimental error when Cl^- was replaced by ClO_4^-. This indicates that the pyridinium and methylimidazolium chlorides **1–4** exist as solvent-separated ion pairs in polar solvents.

3.5. Theoretical calculations

In order to obtain a better insight into the properties of the lowest excited singlet states, a theoretical investigation of molecules **1–4** was undertaken by means of the standard INDO/S CI [27] method. The AM1 [28] and PM3 [29] methods were used for the calculation of the molecular structures in the ground state. The choice of the method and the validity of parametrization were assessed by a comparison of the known crystal structures of the closely related compounds 1,1′-(2,4-pyrimidinediyl)dipyridinium dichloride and 1,1′-(pyrimidine-2-one-4-yl)dipyridinium dichloride [30,31] with those calculated by the MNDO, AM1 and PM3 methods. Very good agreement between the experimental and PM3 calculated structures was found. The ground state potential functions for internal rotation about the C(4)–N (inter-ring) bond of compounds **1–4**, calculated by the PM3 method, are shown in Figs. 4 and 5. The *N*-(pyrimidinyl)pyridinium species **1** and **2** are flexible molecules and can adopt conformations having a broad

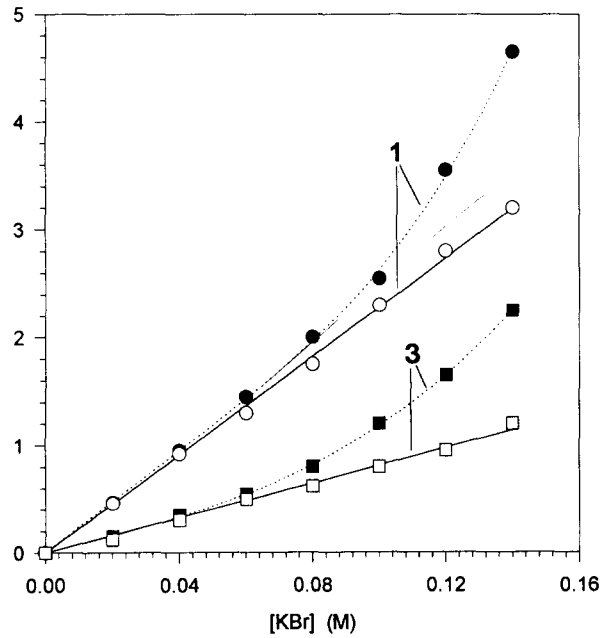

Fig. 3. Stern–Volmer plots for the fluorescence quenching of compounds **1** and **3** by Br^- ions. $\phi^0/\phi - 1$ (●, ■); $\tau^0/\tau - 1$ (○, □).

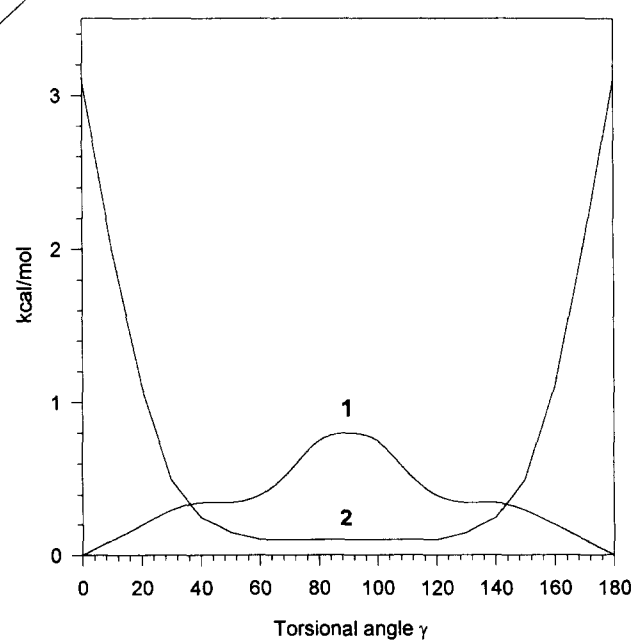

Fig. 4. Potential functions for internal rotation about the C–N inter-ring bond of the pyridinium compounds **1** and **2** in the ground state.

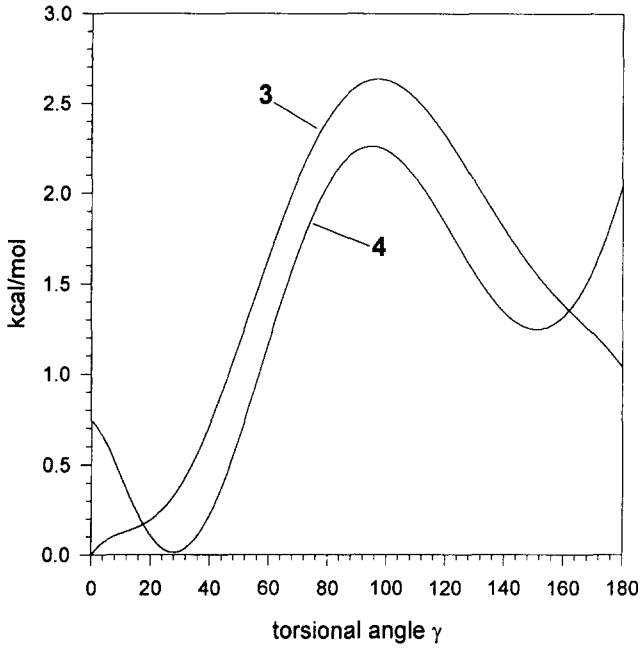

Fig. 5. Potential functions for internal rotation about the C–N interring bond of the methylimidazolium compounds **3** and **4** in the ground state.

range of torsional angles γ. Although a coplanar arrangement of two molecular fragments is calculated to be the lowest energy conformation of **1**, the energy barrier to internal rotation through the perpendicular conformation ($\gamma=90°$) is 0.8 kcal mol^{-1} and is only 0.2 kcal mol^{-1} higher than the thermal energy (kT) at room temperature. In molecule **2**, steric hindrance introduced by the methyl substituent prevents the two rings from assuming coplanar positions, as demonstrated by a steeply rising torsional potential function at $\gamma=0°$. In the equilibrium conformation, the torsional angle equals 67°, but conformations with $50° < \gamma < 130°$ are almost isoenergetic. Molecules **3** and **4** are more rigid, with the energy barrier to internal rotation about the C(6)–N bond being much higher (2 and 2.6 kcal mol^{-1} respectively, see Fig. 5). In the most stable conformation of compound **3**, both heterocyclic rings are coplanar, while in compound **4**, the methylimidazole ring is twisted from the plane of the pyrimidinone ring with $\gamma=28°$.

The energies of the electronic transitions, oscillator strengths and dipole moment changes calculated by the INDO/S method for selected conformations of compounds **1–4** are presented in Table 5. For all the compounds studied, the long-wavelength absorption band is a superposition of four electronic transitions, two of very low oscillator strength. The calculated energy of the first electronic transition is about 1100 cm^{-1} for **1** and 1400 cm^{-1} for **3**, red shifted with respect to the position of the first absorption band measured in butyronitrile. The calculated values of 36 900 cm^{-1} and 37 400 cm^{-1} for the $S_1 \leftarrow S_0$ transition energy in **1** and **2** respectively are in very good agreement with

Table 5
Transition energies, oscillator strengths (f) and dipole moment changes ($\Delta\mu$) calculated for selected conformations of compounds **1–4**

Compound	$\Delta E(S_n \leftarrow S_0)$ (cm^{-1})	f	$\Delta\mu$ (D)
1	27700	0.081	13.65
$\gamma=0°$	29400	0.000	6.51
	32300	0.004	4.55
	33900	0.144	9.19
	36900	0.180	0.12
1	30400	0.001	12.91
$\gamma=90°$	30400	0.001	9.19
	31500	0.229	3.47
	33700	0.004	4.55
	37800	0.194	0.51
2	26200	0.115	13.62
$\gamma=0°$	28400	0.001	6.10
	31700	0.003	4.77
	32400	0.119	8.54
	36600	0.168	0.07
2	28100	0.000	19.09
$\gamma=90°$	30100	0.240	3.08
	30200	0.000	5.41
	33400	0.003	4.24
	37600	0.194	0.27
2	27700	0.033	17.06
$\gamma=67°$	30100	0.002	5.56
	30400	0.205	5.09
	33300	0.005	4.24
	37400	0.185	0.70
3	29300	0.133	9.63
$\gamma=0°$	30100	0.000	5.95
	33000	0.004	4.30
	35400	0.111	11.45
	37000	0.126	5.54
3	30400	0.000	5.23
$\gamma=90°$			
4	28100	0.148	9.62
$\gamma=28°$	29900	0.001	5.86
	32900	0.010	4.10
	33200	0.090	10.50
	37000	0.134	5.31
4	27500	0.154	9.77
$\gamma=0°$			
4	30200	0.183	3.89
$\gamma=90°$			

the experimentally found maxima of the second UV absorption band (37 500 cm^{-1} for **1** and 38 200 cm^{-1} for **2**). The experimentally found spectral shift between the UV absorption maxima of **3** and **4** (1500 cm^{-1}) is well reproduced by the calculation (1200 cm^{-1}). In the case of **1** and **2**, in contrast with the experimental observation, no shift is predicted theoretically assuming the planar structure ($\gamma=0°$) for **1** and the twisted structure ($\gamma=67°$) for **2**. This inconsistency may indicate that, in solution, the two heterocyclic rings in **1** deviate from planarity. The energies of the first electronic

transitions in the perpendicular conformers ($\gamma = 90°$) of compounds **1** and **2** are higher by 2700 cm^{-1} (7.7 kcal mol^{-1}) and 1900 cm^{-1} (5.4 kcal mol^{-1}) respectively than those in the planar conformations. These values, together with the rotational energy barriers presented in Fig. 4, indicate that the perpendicular arrangement of two heterocycle rings in these molecules is not favoured (by about 7 kcal mol^{-1} for **1** and 2 kcal mol^{-1} for **2**) in the singlet excited state. The geometries of compounds **3** and **4** do not change on excitation and the energy barrier to internal rotation at $\gamma = 90°$ becomes higher than that in the ground state. The lowest energy transitions in the compounds studied are associated with a significant charge shift (cf. the large dipole moment changes, Table 5) from the pyrimidinyl to the pyridinium moiety. In the case of **1** and **2**, the charge shift on excitation is 0.6*e*, and this value is essentially independent of the torsional angle γ. In the methylimidazoline cations, the charge shift is smaller at 0.4*e*.

4. Conclusions

Substituent and solvent effects and theoretical calculations show that the lowest energy singlet excited states of the pyridinium (**1** and **2**) and methylimidazolium (**3** and **4**) compounds have significant charge transfer character. Theoretical estimates of the charge shift on excitation from the pyridinium or methylimidazolium moiety to the pyrimidinone group are, however, smaller than those found in the theoretical study of the systems in which exactly one electron is transferred [25]. On excitation, *N*-(pyrimidinyl)pyridinium molecules **1** and **2** undergo relaxation towards more planar arrangements of heterocyclic rings. We suggest, as shown previously for other pyridinium species [3,5], that the rotational relaxation and solvent reorientational effect associated with significantly different charge distribution in the excited states are responsible for the large Stokes shifts found in the spectra of **1** and **2**.

The twisted intramolecular charge transfer (TICT) state, with perpendicular arrangements of the donor and acceptor residues of molecules **1** and **2** is unlikely to be the emitting state, as might be expected taking into account the unusually large Stokes shift. The high values of the transition dipole moments of the emitting states (Table 1) of **1** and **2** and the theoretical studies do not fit this model. Moreover, TICT states in various organic cations, including dyes, are found to be non-emissive [7,25] because they are an efficient channel for non-radiative decay. A similar process could be responsible for the increased values of the non-radiative rate constants in the case of the *N*-(pyrimidinyl)pyridinium species **1** and **2**. This would be consistent with the observed increase in Σk_{nr} by an order of magnitude in the pyridinium derivative **2**, with steric hindrance to planarity.

Acknowledgement

The financial support from the Polish Research Committee (project PN 1031/92/02) is gratefully acknowledged.

References

[1] U.C. Yoon, S.L. Quillen, P.S. Mariano, R. Swanson, J.L. Stavinoha and E. Bay, *J. Am. Chem. Soc., 105* (1983) 1204.
[2] J. Kotlicka and Z.R. Grabowski, *J. Photochem., 11* (1979) 413.
[3] M.I. Knyazhanskii, Y.R. Tymyanskii, V.M. Feigelman and A.R. Katritzky, *Heterocycles, 26* (1987) 2963.
[4] G.M. Backburn, G. Lockwood and V. Solan, *J. Chem. Soc., Perkin Trans. II,* (1976) 1452.
[5] V.A. Kharlanov, M.I. Knyazhaskii, N.I. Makarova and V.A. Lokshin, *J. Photochem. Photobiol. A: Chem., 70* (1993) 70.
[6] H. Ephardt and P. Fromherz, *J. Phys. Chem., 93* (1989) 7717.
[7] P. Fromherz and A. Heilemann, *J. Phys. Chem., 96* (1992) 6864.
[8] W. Abraham, A. Henrion and D. Kreysig, *J. Photochem., 35* (1986) 311.
[9] B. Skalski, R.P. Steer and R.E. Verrall, *J. Am. Chem. Soc., 110* (1988) 2055.
[10] B. Skalski, S. Paszyc, R.W. Adamiak, R.P. Steer and R.E. Verrall, *Can. J. Chem., 68* (1990) 2164.
[11] R.W. Adamiak, E. Biala and B. Skalski, *Nucleic Acids Res., 13* (1985) 2989.
[12] G. Wenska, B. Skalski and Z. Gdaniec, *Can. J. Chem., 70* (1992) 856.
[13] S. Mielewczyk, G. Dominiak, Z. Gdaniec, E. Krzymanska-Olejnik and R.W. Adamiak, *Nucleosides Nucleotides, 10* (1991) 263.
[14] D.F. Eaton, *Pure Appl. Chem., 60* (1988) 1107.
[15] D.V. O'Connor and D. Philips, *Time Correlated Single Photon Counting,* Academic Press, London, 1984.
[16] D.J.S. Birch, G. Hungerford and R.E. Imhof, *Rev. Sci. Instrum., 62* (1991) 2405.
[17] J.B. Birks, *Photophysics of Aromatic Molecules,* Wiley Interscience, New York, 1970.
[18] B. Skalski, S. Paszyc, R.W. Adamiak, R.P. Steer and R.E. Verrall, *J. Chem. Soc., Perkin Trans. II,* (1989) 1691.
[19] E. Lippert, *Z. Electrochem., 61* (1957) 962.
[20] L. Bilot and A. Kawski, *Z. Naturforsch., Teil A, 17* (1962) 621.
[21] O. Kasende and Th. Zeegers-Huyskens, *J. Phys. Chem., 88* (1984) 2636.
[22] M.J. Kamlet, J.-L.M. Abboud, M.H. Abraham and R.W. Taft, *J. Org. Chem., 48* (1983) 2877.
[23] W. Kupfer and W. Abraham, *J. Prakt. Chem., 325* (1983) 95.
[24] C. Parkanyi, C. Boniface, J.J. Aaron and M. Maafi, *Spectrochim. Acta, Part A, 49* (1993) 1715.
[25] W. Rettig, *Angew. Chem., Int. Ed. Engl., 25* (1986) 971.
[26] A.I. Tolmachov, A.K. Zaitsev, N. Koska and G.B. Schuster, *J. Photochem. Photobiol. A: Chem., 77* (1994) 237.
[27] J. Ridley and M. Zerner, *Theor. Chim. Acta, 42* (1971) 223.
[28] M.J.S. Dewar, E.G. Zoebish, E.F. Healy and J.J.J. Steward, *J. Am. Chem. Soc., 107* (1985) 3902.
[29] J.J.P. Stewart, *J. Comput. Chem., 10* (1989) 209.
[30] M. Jaskolski, B. Skalski and D. Adamiak, *Acta Crystallogr., Sect. C, 44* (1988) 1409.
[31] K. Surma, D. Adamiak, M. Gawron and B. Skalski, *Acta Crystallogr., Sect. C, 48* (1992) 298.